Non-classical Ly6C^{-} monocytes drive the development of inflammatory arthritis in mice.

Alexander V Misharin, Carla M Cuda, Rana Saber, Jason D Turner, Angelica K Gierut, G. Kenneth Haines, Sergejs Berdnikovs, Andrew Filer, Andrew R Clark, Christopher D Buckley, Gökhan M Mutlu, G.R. Scott Budinger, Harris Perlman

Supplemental experimental procedures

Bone marrow chimeras and shielded bone marrow chimeras

CD11b-DTR and CD11c-DTR mice do not survive multiple injections of diphtheria toxin (data not shown). Bone marrow chimeras were established by transferring $5x10^6$ bone marrow cells isolated from CD11b-DTR or CD11c-DTR mice (all strains express CD45.2 alloantigen) into 8-week-old lethally irradiated (single dose of 1000 cGy γ-radiation using a Cs-137 based Gammacell-40 irradiator (Nordion)) recipient mice (expressing CD45.1 alloantigen). Mice were maintained on autoclaved water supplemented with antibiotics (Trimetoprim/Sulfamethoxazole, Hi-Tech Pharmacal) for 4 weeks after bone marrow transfer and then switched to normal housing regimen. CD11b-DTR(CD45.2)→WT(CD45.1) and CD11c-DTR(CD45.2)→WT(CD45.1) bone marrow chimeras were used for experiments 8 weeks after bone marrow transfer. Eight weeks after bone marrow transfer more than 95% of all leukocytes and 100% of monocytes and neutrophils in peripheral blood were of donor origin. Shielded bone marrow chimeras were used to assess local proliferation of tissue-resident synovial macrophages in the steady state and during STIA. To ensure that tissue-resident synovial macrophages are not damaged during the irradiation, we protected them with the lead strips. To completely ablate recipient's bone marrow (CD45.2) in the shielded ankles, 12 hours after shielded irradiation mice received myeloablative agent busulfan (30 mg/kg), donor's bone marrow (CD45.1) was transplanted 12 hours later. Shielded bone marrow chimeras were maintained on antibiotics for 4 weeks as described above. Six weeks later, 100% of the circulating monocytes were of donor origin.

Diphtheria toxin treatment and monocyte depletion

To deplete peripheral blood monocytes and tissue macrophages, diphtheria toxin (Sigma) in 200 μL of PBS was administered intraperitoneally, at the indicated time points and doses 10 ng/g (for CD11b-DTR) or 4 ng/g (for CD11c-DTR) body weight. Control mice were treated with vehicle (PBS). Monocytes in peripheral blood were depleted by intravenous injection of 200 μL of clodronate-loaded liposomes (purchased from http://www.clodronateliposomes.com). Control animals received PBS-loaded liposomes. To track cells that

uptake the liposomes, PBS-loaded liposomes labeled with DiD fluorescent dye (Invitrogen) were used. Classical ($Ly6C^+$) monocytes in peripheral blood were depleted by intravenous injection of 6 μg of anti-CCR2 antibody (clone MC-21) at the indicated time points.

Histopathology scoring

The following criteria were used for inflammation: 0 – normal; 1 – minimal infiltration of inflammatory cells in periarticular tissue; 2 – mild infiltration; 3 – moderate infiltration, with moderate edema; 4 – marked infiltration, with marked edema; and 5 – severe infiltration, with severe edema. Pannus formation was scored according to the following criteria: 0 – normal; 1 – few pannus formation at 1 to 2 position; 2 – moderate pannus formation at 1 to 2 position; 3 – pronounced pannus formation with accretion to cartilage; 4 – pronounced pannus formation with cartilage overgrow; 5 – pronounced cartilage destruction due to pannus invasion. Bone erosion was scored according to the following criteria: 0 – normal; 1 – Small areas of resorption, not readily apparent on low magnification, in trabecular or cortical bone; 2 – More numerous areas of resorption, not readily apparent on low magnification, in trabecular or cortical bone; 3 – Obvious resorption of trabecular and cortical bone, without full thickness defects in the cortex; loss of some trabeculae; lesions apparent on low magnification; 4 – Full thickness defects in the cortical bone and marked trabecular bone loss, without distortion of the profile of the remaining cortical surface; 5 – Full thickness defects in the cortical bone and marked trabecular bone loss, with distortion of the profile of the remaining cortical surface. Microphotographs were taken on Olympus BX41 and Nikon Eclipse TE2000E2 microscopes.

Histology and histopathology

Ankles were fixed in formalin, decalcified in 7% EDTA, processed for histology (haematoxylin and eosin) and immunohistochemistry (F4/80, clone BM8). Slides were scored by a pathologist (G.K.H.) blinded to the study. Tibiotalar joints scored separately for bone erosion, inflammation, pannus formation and infiltration with specific cell subsets (see Supplemental experimental procedures for scoring criteria). Microphotographs were

taken on Olympus BX41 and Nikon Eclipse TE2000E2 microscopes. Immunofluorescent microscopy described in Supplemental experimental procedures.

Immunofluorescent microscopy on mouse tissues

Ankles from one day-old mice were snap-frozen in Tissue-Tek (Sakura Finetek) and 10 μm sections were prepared on Cryocut 1800 cryostat (Reichert Microscope Services). Sections were fixed in acetone, blocked with FcBlock and rat serum, and stained with CD11b-Brilliant Violet 421 (Biolegend), CD64-PE (Biolegend), CD206-Alexa Fluor 647 (AbdSerotech), F4/80-Alexa Fluor 647 (AbdSerotech), MHC II-FITC (eBioscience) antibodies. Nuclei were visualized by staining with DAPI (Invitrogen). Images were acquired on Nikon A1R microscope at Northwestern University Cell Imaging core facility.

Immunofluorescent microscopy on human synovial tissue

Synovial tissues were obtained from individuals with mechanical joint symptoms undergoing exploratory arthroscopy during which no evidence of synovial pathology was found macroscopically or on subsequent histological analysis or from patients with RA undergoing the joint replacement. The study was approved by The west Midlands Black Country Research Ethics Committee (Reference 07/H1204/191). All patients gave written informed consent to participate. Tissues from biopsies or joint replacements were mounted in OCT compound (Tissue-Tek) and frozen in the gas phase of liquid nitrogen. Sections were cut on a cryostat at 6μm thickness. They were subsequently air-dried and fixed for 20 minutes in acetone (J.T.Baker) in 4C. Sections were blocked in PBS v/v 10% FCS for 10 minutes then stained with primary antibodies overnight at 4C (see Supplemental Table S3). Slides were washed in PBS and stained with secondary antibodies for 1 hour at room temperature. After another PBS wash slides were counterstained with 4μg/ml Hoechst 33258, Pentahydrate (bis-Benzimide) (Invitrogen) for 20 minutes before undergoing a final wash with PBS. Slides were mounted with 2.4% w/v 1,4-diazabicyclo (2,2,2) octane (Sigma Aldrich) in 90% v/v glycerol (Sigma Aldrich) in PBS (pH, 8.6). Images were acquired using a 40x objective on an LSM 510 confocal microscope running LSM 510

version 3.2 SP2 software (Carl Zeiss). FITC conjugates were excited with a 488nm argon laser, Cy3 conjugates with a 543nm HeNe laser, Cy5 conjugates with a 633nm helium laser, and the nuclear counterstain Hoechst with 351/364 lasers. Fluorescence was captured in single channels and merged by the software after acquisition. Representative single channel and merged images were exported as TIFF files using ZEN black 2010 (Carl Zeiss) and images for figures were generated using ImageJ (NIH). No further image manipulations were undertaken.

Isolation and adoptive transfer of monocytes

To isolate monocytes from splenic pool single cell suspension was prepared as described above. Bone marrow was harvested from femurs and tibias, filtered through 40 μm nylon mesh, and erythrocytes were lysed using BD Pharm Lyse (BD Biosciences). Single cell suspension from spleen and bone marrow was stained with anti-CD115-PE antibody following anti-PE microbeads (Miltenyi) and enriched on AutoMACS (Miltenyi) instrument. CD115-enriched fraction was stained with a mixture of fluorochrome-conjugated antibodies and classical $Ly6C^+$ and non-classical ($Ly6C^-$) monocytes were sorted on FACSAria III instrument. Splenic monocytes were identified as Lin^-(CD4, CD8, CD11c, CD19, NK1.1, Ly6G, Siglec F, MHC II)$CD11b^+CD115^+F4/80^{low}$, bone marrow monocytes were identified as $Lin^-CD117^-Sca\text{-}1^-CD11b^+CD115^+$. $1x10^6$ of classical $Ly6C^+$ monocytes or $0.5x10^6$ of non-classical $Ly6C^-$ monocytes were adoptively transferred intravenously via retro-orbital injection.

Supplemental data

Table S1. **Antibodies used for flow cytometric analysis** (see Methods: Flow cytometry). APC is allophycocyanin, FITC is fluorescein isothiocyanate, PE is R-Phycoerythrin, PerCP is Peridinin Chlorophyll.

Antigen	**Clone**	**Fluorochrome**	**Manufacturer**
CD11b	M1/70	eFluor 450 PerCPCy5.5	eBioscience
CD11c	HL3	PE-Cy7	BD Biosciences
CD16	275003	APC	R&D
CD32b	190907	APC	R&D/Innova Bioscience
CD36	CRF D-2712	APC	BD Biosciences
CD40	HM40-3	Alexa Fluor 647	Biolegend
CD45	30-F11	FITC eFluor 450	eBioscience
CD64	X54-5/7.1	PE APC	Biolegend
CD80	16-10A1	APC	BD Biosciences
CD86	GL1	APC	BD Biosciences
CD206	MR5D3	Alexa Fluor 647	AbD Serotec
F4/80	Cl:A3-1	Alexa Fluor 647	AbD Serotec
Ly6G	1A8	Alexa Fluor 700 PECF594 PECy7	BD Biosciences BD Biosciences Biolegend
Ly6C	AL-21	APC-Cy7 FITC	BD Biosciences
MHC II (I-A/I-E)	M5/114.15.2	eFluor450 PerCPCy5.5	eBioscience Biolegend
Siglec F	E50-2440	APC PE	BD Biosciences

		Horizon PE-CF594	
RELMa	Rabbit polyclonal	Alexa Fluor 647	PeproTech/Invitrogen
TLR2	6C2	APC	eBioscience
TLR4	MTS510	APC	eBioscience
Tim-4	RMT4-54	APC PE	Biolegend
MerTK	BAF591	APC	R&D
TNFa	MP6-XT22	PECy7	Biolegend
IL-10	JES5-16E3	PE	eBioscience
IL-1b	NJTEN3	eFluor450	eBioscience

T**able S2**: **Configuration of the BD LSR II instrument** (see Methods: Flow cytometry).

Laser	**Detector**	**Filter**	**Mirror**	**Fluorochromes**
Blue (488 nm)	A	710/50	685LP	PerCP-Cy5.5
	B	525/50	505LP	FITC GFP
Red (640 nm)	A	780/60	735LP	APC-Cy7
	B	730/45	690LP	Alexa Fluor 700
	C	670/30		APC Alexa Fluor 647
Yellow-green (561 nm)	A	780/60	735LP	PE-Cy7
	B	610/20	600LP	PE-Texas Red Horizon PE-CF594
	C	582/15		PE
Violet (405 nm)	A	525/50	550LP	Horizon V500 Aqua Live/Dead eFluor 506 Live/Dead
	B	450/50		eFluor 450 Brilliant Violet 421

Table S3. Antibodies used for immunofluorescent microscopy on human synovial tissue (See Supplemental Methods: Immunofluorescent microscopy on human synovial tissue and Figure S2).

Primaries

Marker	Working dilution	Clone	Isotype	Supplier
CD163	1/450 (2.22µg/ml)	EDHu-1	Mouse IgG1	AbD Serotec
CD68	1/100 (5µg/ml)	Y1/82A	Mouse IgG2b, κ	BD Biosciences
HLA-DR	1/50	L243	Mouse IgG2a, κ	BD Biosciences

Secondaries

Marker/Target	Conjugate	Working dilution	Isotype	Supplier
Anti-Mouse IgG1	FITC	1/50 (10 µg/ml)	Goat IgG	SouthernBiotech
Anti-Mouse IgG2a	TRITC	1/50 (20 µg/ml)	Goat IgG	SouthernBiotech
Anti-Mouse IgG2b	Cy5	1/250 (4 µg/ml)	Goat IgG	SouthernBiotech

Table S4: Affymetrix QuantiGene 2.0 custom panel #21522 for analysis of macrophage polarization (See Methods: Analysis of macrophage polarization and Figure 7).

	Protein	Gene	GeneBank Accession #	Role
1	NO synthetase	*Nos2*	NM_010927	M1
2	RELMα	*Retnla*	NM_020509	M2
3	Ym-1	*Chi3l3*	NM_009892	M2
4	Arginase	*Arg1*	NM_007482	M2
5	Tissue Transglutaminase 2	*Tgm2*	NM_009373	M2
6	Transferrin Receptor (CD71)	*Tfrc*	NM_011638	M2
7	Sphingosine kinase 1	*Sphk1*	NM_011451	M2
8	Tumor necrosis factor (ligand) superfamily, member 14	*Tnfsf14*	NM_019418	M2
9	Heparin-binding EGF-like growth factor	*Hbegf*	NM_010415	M2
10	FcyRIIb (CD32b)	*Fcgr2b*	NM_010187	M2
11	FcyRI (CD64)	*Fcgr1*	NM_010186.5	M1
12	CD163	*Cd163*	NM_053094	M2
13	CD36	*Cd36*	NM_007643	M2
14	Mannose Receptor (CD206)	*Mrc1*	NM_008625	M2
15	IL-12-p40	*IL12b*	NM_008352	M1
16	IL-12-p70	*IL12a*	NM_008351	M1
17	IL-10	*Il10*	NM_010548	M2
18	TGFbeta1	*Tgfb1*	NM_011577	M2
19	CXCL13	*Cxcl13*	NM_018866	M2
20	IL-6	*Il6*	NM_031168	M1
21	IL-23 (p19)	*Il23a*	NM_031252	M1
22	IL-1 beta	*Il1b*	NM_008361	M1
23	TNF	*Tnf*	NM_013693	M1
24	SOCS1	*Socs1*	NM_009896	M2
25	SOCS3	*Socs3*	NM_007707	M2
26	Nur77	*Nr4a1*	NM_010444	M2
27	JMJD3	*Kdm6b*	NM_001017426	M2
28	IRF4	*Irf4*	NM_013674	M2
29	IRF5	*Irf5*	NM_012057	M1

30	IRF8	*Irf8*	NM_008320	M1
31	PPARγ	*Pparg*	NM_011146	M2
32	SHIP	*Inpp5d*	NM_010566	M2
33	STAT6	*Stat6*	NM_009284	M2
34	P21	*Cdkn1a*	NM_007669	
35	KLF4	*Klf4*	NM_010637	M2
36	CARKL	*Shpk*	NM_029031	M2
37	NF-kB1 (p50)	*Nfkb1*	NM_008689	M1
38	C/EBPbeta	*Cebpb*	NM_009883	M2
39	Akt1	*Akt1*	NM_001165894	M2
40	Akt2	*Akt2*	NM_001110208	M1
41	IL-4R (CD124)	*Il4ra*	NM_001008700	M2
42	M-CSF (CD115)	*CSF1R*	NM_001037859	
43	GM-CSFR (CD116)	*CSF2RA*	NM_009970	
44	Tim-4	*Timd4*	NM_178759	M2
45	MerTK	*Mertk*	NM_008587	M2
46	PTEN	*Pten*	NM_008960	M1
47	IL-1RA	*Il1rn*	NM_001039701	M2
48	CD80	*CD80*	NM_009855	M1
49	CD86	*CD86*	NM_019388	M2
50	CCL17	*Ccl17*	NM_011332	M2
51	IL-33	*Il33*	NM_001164724	M2
52	CD39	*Entpd1*	NM_009848	M2
53	peptidylprolyl isomerase B	*Ppib*	NM_011149	housekeeping
54	ATPase, H+ transporting, lysosomal V1 subunit A	*Atp6v1a*	NM_007508	housekeeping
55	thioredoxin nuclear gene encoding mitochondrial protein	*Txn2*	NM_019913	housekeeping
56	hypoxanthine guanine phosphoribosyl transferase	*Hprt*	NM_013556	housekeeping
57	succinate dehydrogenase complex, subunit A, flavoprotein	*Sdha*	NM_023281	housekeeping
58	polymerase (RNA) II (DNA directed) polypeptide A	*Polr2a*	NM_009089	housekeeping

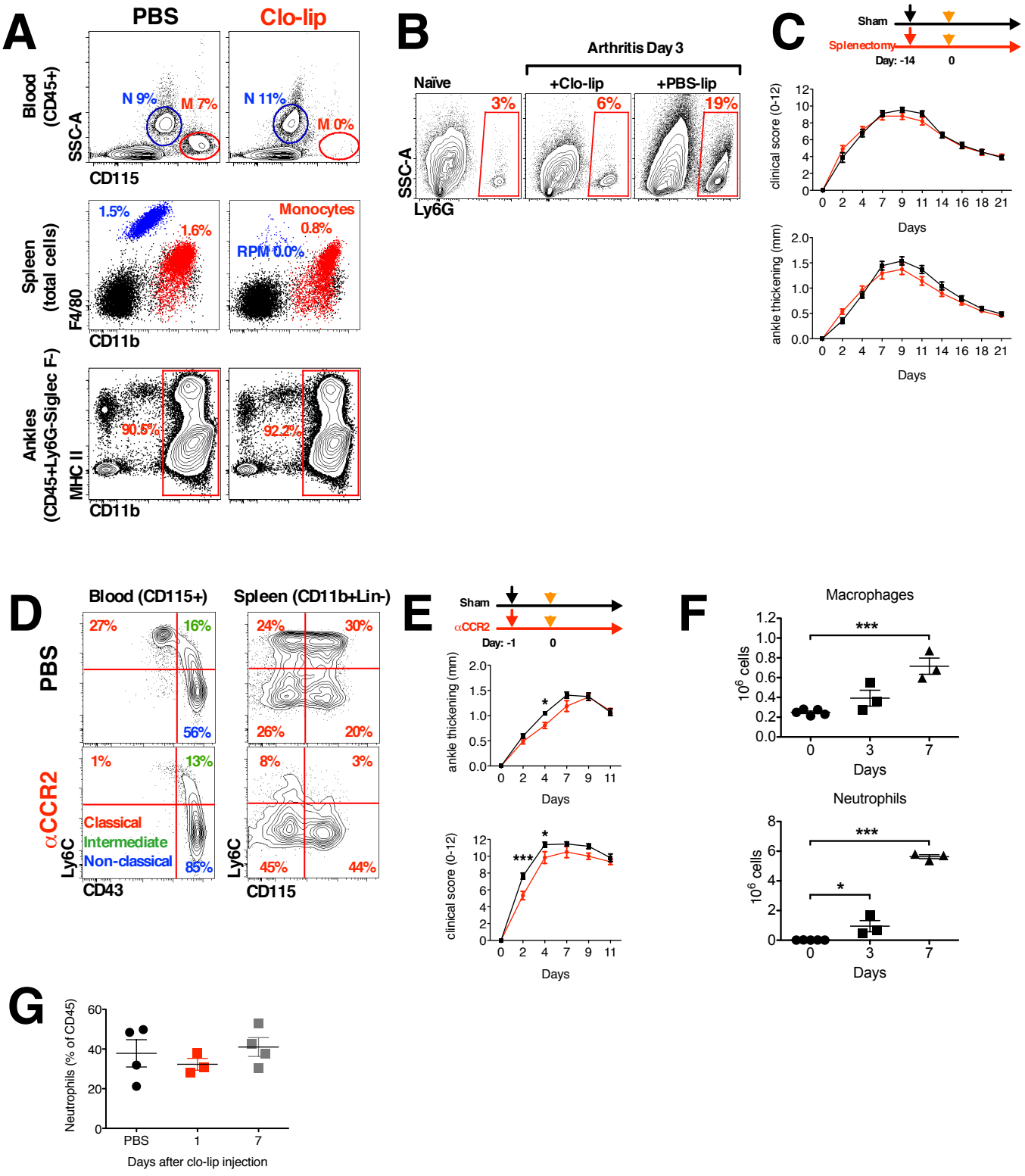

Figure S1. Role of monocytes in the initiation and development of serum transfer arthritis (see Figure 1).

A. Top panel: Single intravenous injection of clodronate-loaded liposomes depletes all circulating monocytes

(M) in blood and does not affect neutrophils (N). Representative contour plots gated on CD45+ cells are shown (numbers indicate percentage of the parent population). Middle panel represents number of monocytes in the splenic pool ($CD11b^{+}F4/80^{low}CD11c^{-}MHC\ II^{-}NK1.1^{-}Ly6G^{-}Siglec\ F^{-}$) and red pulp macrophages ($F4/80^{+}CD11b^{-}$). Red pulp macrophages (blue) and splenic monocytes (red) shown as overlays on CD11b vs. F4/80 dot plot (numbers indicate percentage of the total splenic cells). Bottom panel: Clodronate-loaded liposomed do not affect the number of synovial macrophages (defined as $CD45^{+}CD11b^{+}Ly6G^{-}Siglec\ F^{-}$ cells). Representative contour plots gated on are shown, numbers indicate percentage of the parent population. B. Depletion of monocytes prevents neutrophil recruitment into ankles. Representative contour plots are shown (numbers indicate percentage of the parent ($CD45^{+}$) population). Left panel represents naïve mice, middle panel represents mice treated with clodronate-loaded liposomes 3 days after induction of STIA and right panel represents mice treated with PBS-loaded liposomes 3 days after induction of STIA. C. Splenectomy does not affect number the course of STIA. Splenectomy (n = 10) or sham procedure (n = 9) was performed and STIA was induced two weeks later. D. Anti-CCR2 antibody eliminates classical $Ly6C^{+}$ monocytes in circulation ($CD115^{+}$, left panel) and splenic pool ($CD11b^{+}F4/80^{low}CD11c^{-}MHC\ II^{-}NK1.1^{-}Ly6G^{-}Siglec\ F^{-}$, right panel). Representative contour plots are shown (numbers indicate percentage of the parent population). E. Depletion of classical Ly6C+ monocytes does not affect the initiation and propagation of STIA (n = 6). F. $CCR2^{-/-}$ mice recruit both neutrophils and macrophages into the joins during STIA (n = 3-5). One-way ANOVA with Dunnett's multiple comparison test was used to analyze difference between populations. G. Injection of clodronate-loaded liposomes does not affect the number of circulating neutrophils. All data are represented as mean ± SEM. Differences between the groups were compared using two-way ANOVA for repeated measurements, with Bonferroni post-test, * $p<0.05$, ** $p<0.01$, *** $p<0.001$.

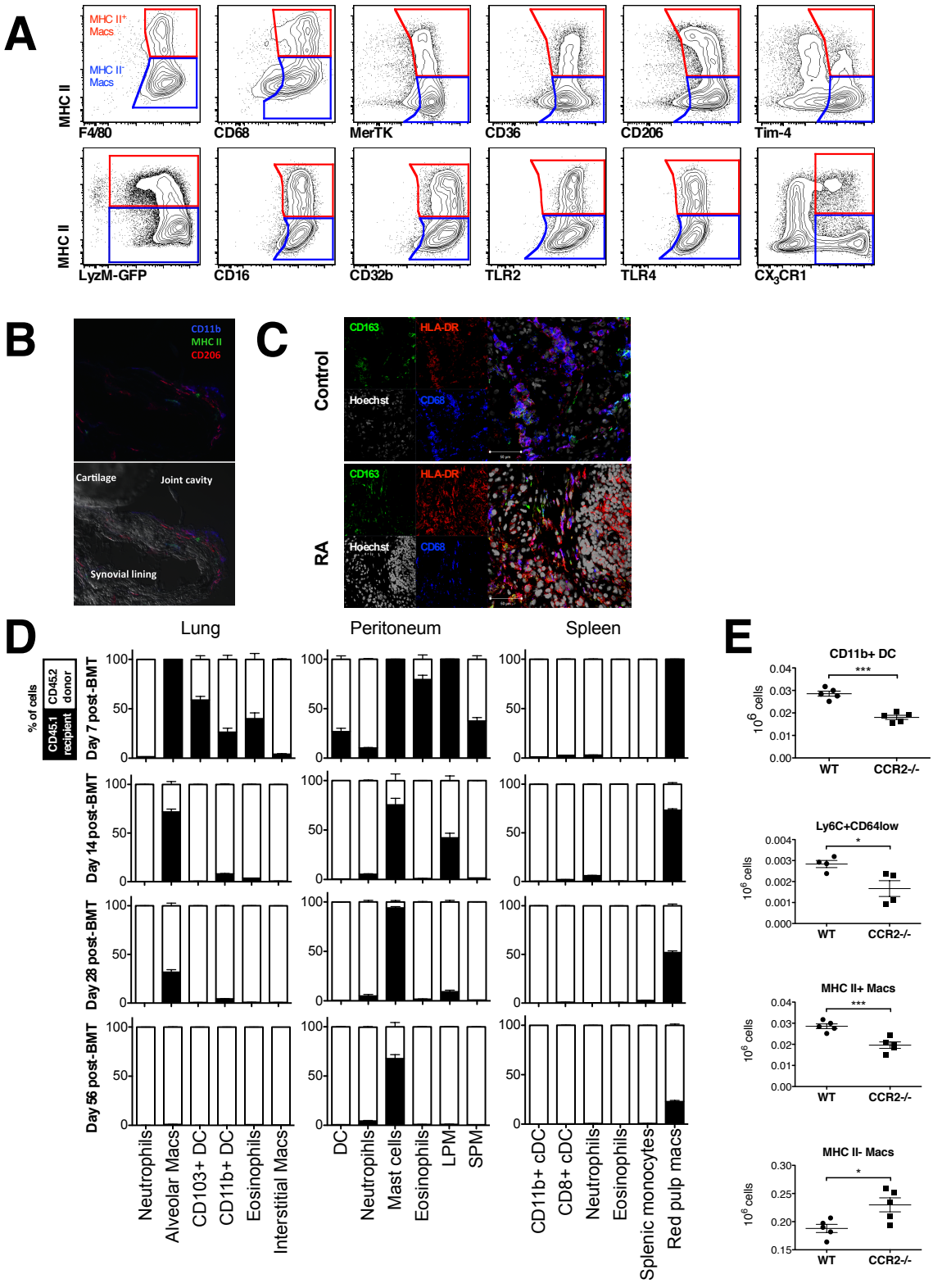

Figure S2. Characterization and origin of synovial macrophages (see Figure 2).

A. Characterization of synovial macrophages using flow cytometry. Representative contour plots are shown

(gated on macrophages). Red gates show MHC II^+ and blue gates show MHC II^- macrophages positive for a given marker. B. Immunofluorescent microscopy of the cryostat sections of mouse ankles. Top panel represents fluorescence and right panel represents merge of fluorescence and bright field image. Blue: CD11b-Brilliant Violet 421. Green: MHC II-FITC. Red: CD206-AF647. $CD11b^+CD206^+$ cells are localized in synovial lining and joint capsule. C. Immunofluorescent microscopy of the cryostat sections of the healthy (top panel) and RA (bottom panel) human synovial tissue. Green: CD163. Red: HLA-DR. Blue: CD68. White: Hoechst. $CD68^+CD163^+HLA\text{-}DR^-$ cells are turquoise, $CD68^+CD163^-HLA\text{-}DR^+$ cells are purple. D. Replacement of different myeloid populations was followed over the course of eight weeks in CD45.2→CD45.1 bone marrow chimeric mice (n = 4). E. Subpopulations of the myeloid cells in the synovium of WT and CCR2-/- mice (n = 5). All data are represented as mean ± SEM. Differences between the groups were compared using paired two-tailed t-test.

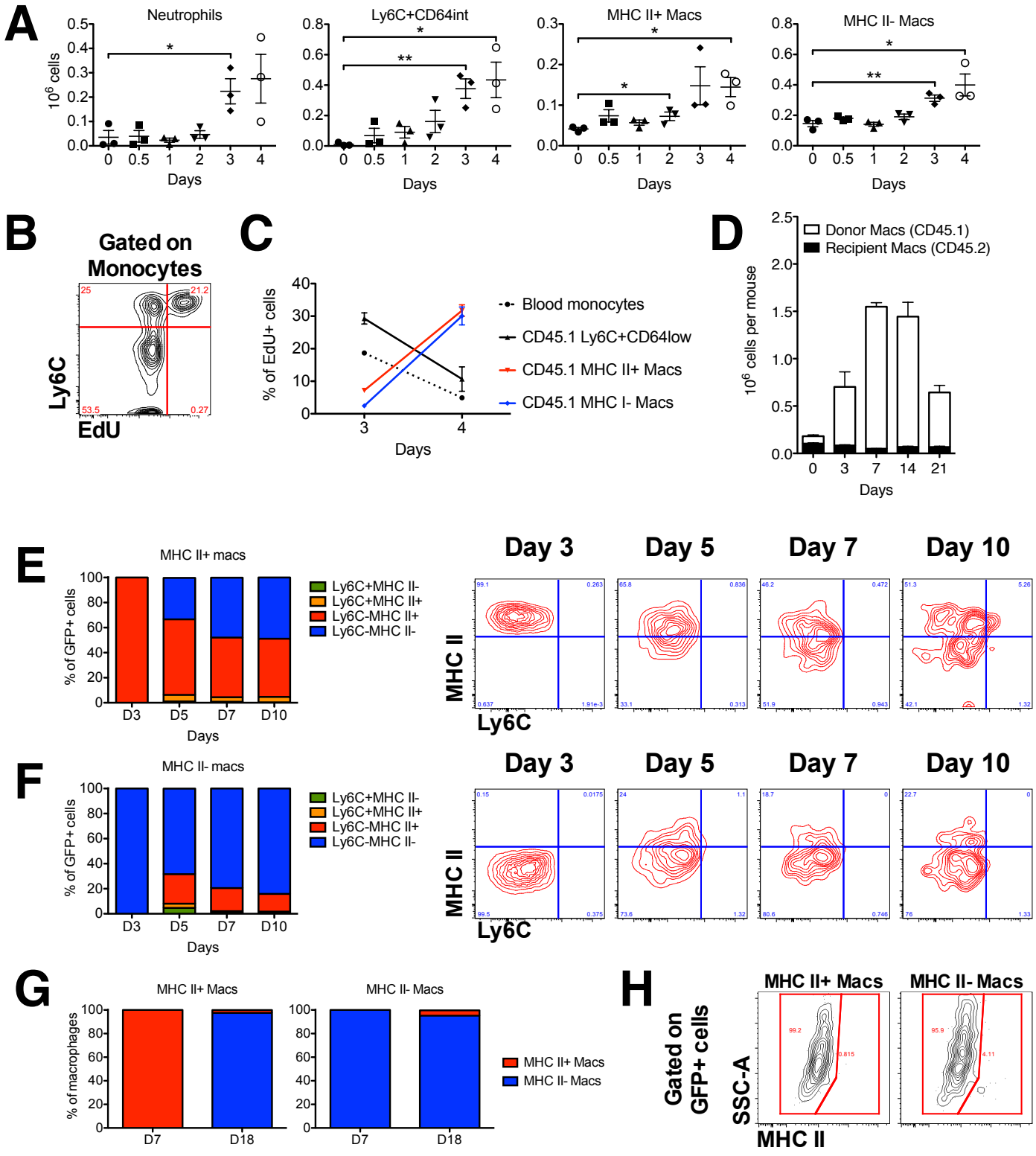

Figure S3. Steady state MHC II$^+$ macrophages exhibit phenotypic plasticity (see Figure 3).

A. Dynamics of the myeloid cell subsets during early phase of STIA (n = 3). B. Twenty-four hours after

injection of 2 mg EdU only classical Ly6C+ monocytes acquire the label. C. Percentage of EdU+ blood monocytes and myeloid cell subsets 24 (Day 3) and 48 hours (Day 4) after 2 mg pulse with EdU (n = 3). D. Number of recipient (tissue-resident) macrophages does not significantly change during the course of STIA (n = 4). E-F. Fate macrophages during the course of STIA. GFP-positive MHC II+ (E) and MHC II- (F) macrophages were sorted from day 3 STIA ankles of CX_3CR1-gfp reporter mice and adoptively transferred into periarticular space of day 3 STIA mice. Phenotype of the transferred cells (GFP^+) was analyzed 2, 4 and 7 days after the transfer. Bar graphs represent percentages of the GFP^+ cells with specific phenotype (n = 3). Representative contour plots gated on macrophages are shown (numbers indicate percentages of the parent population). G-H. Fate of macrophages during the course of STIA. GFP-positive MHC II+ and MHC II- macrophages were sorted from day 7 STIA ankles of CX_3CR1-gfp reporter mice and adoptively transferred into periarticular space of day 7 STIA mice. Phenotype of the transferred cells (GFP^+) was analyzed 11 days after the transfer (STIA day 18). Bar graphs represent percentages of the GFP^+ cells with specific phenotype (n = 4-5). Representative contour plots gated on adoptively transferred macrophages are shown (numbers indicate percentages of the parent population).

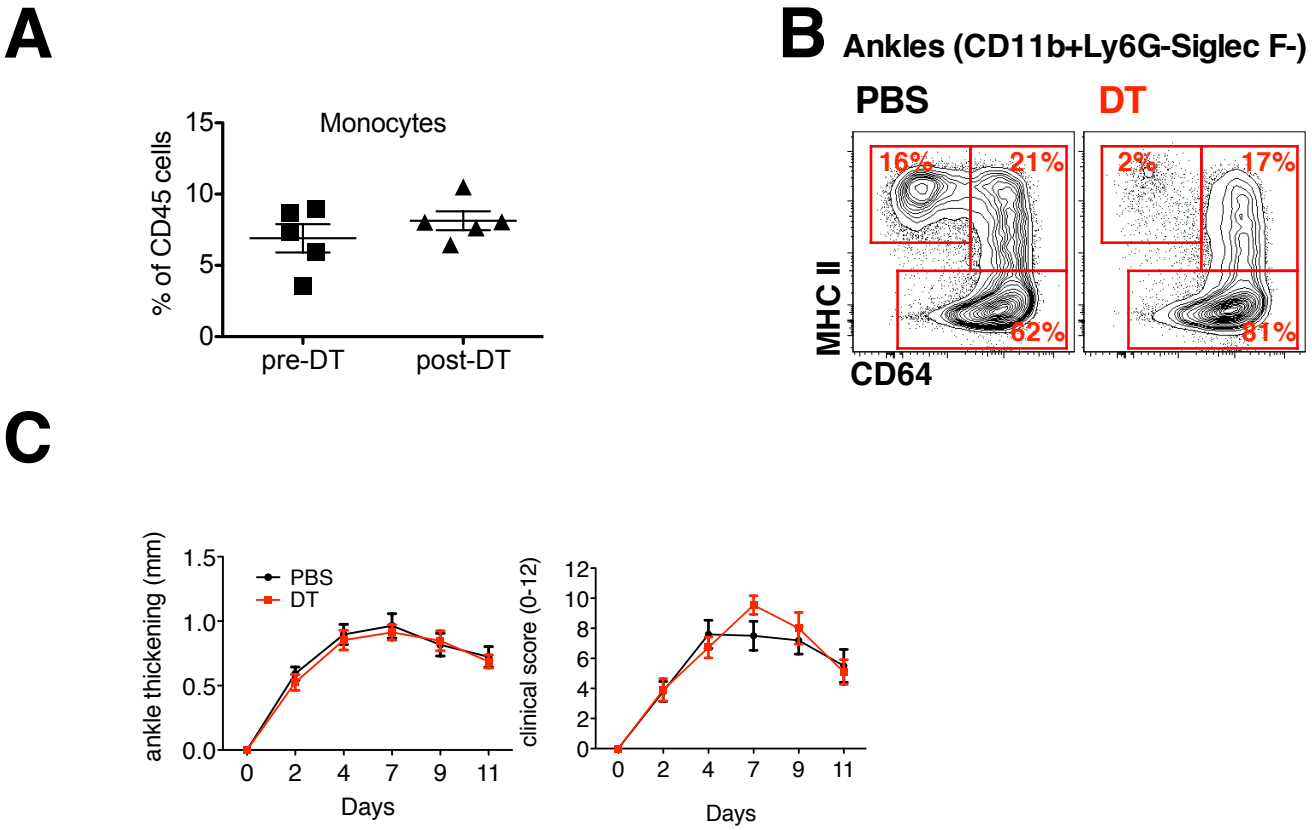

Figure S4. CD11c^{+} DCs are not required for STIA (see Figure 4).

A. Local injection of DT does not affect circulating monocytes. Peripheral blood was collected before and 24 hours after local injection of DT. Monocytes were determined as CD45^{+}CD115^{+} cells via flow cytometry. B. DT depletes CD11b+ DC in the synovium of CD11c-DTR mice and has minimal effect on MHC II^{+} macrophages and does not affect MHC II^{-} macrophages. Representative contour plots are shown (numbers indicate percentage of the parent population). C. Administration of DT to CD11c-DTR → CD45.1 bone marrow chimeric mice does not affect the course of STIA (n = 11). All data are represented as mean ± SEM. Differences between groups were compared using two-way ANOVA for repeated measurements, with Bonferroni post-test, * $p<0.05$, ** $p<0.01$, *** $p<0.001$.